pISSN 2384-1095
eISSN 2384-1109

iMRI 2017;21:1-8

https://doi.org/10.13104/imri.2017.21.1.1

iMRI
Investigative Magnetic Resonance Imaging

Dual Component Analysis for *In Vivo* T_2* Decay of Hyperpolarized ^{13}C Metabolites

Eunhae Joe[1], Joonsung Lee[2], Hansol Lee[1], Seungwook Yang[1], Young-Suk Choi[3], Eunkyung Wang[3], Ho-Taek Song[3], Dong-Hyun Kim[1]

[1]Department of Electrical and Electronic Engineering, Yonsei University, Seoul, Korea
[2]Center for Neuroscience Imaging Research, Institute for Basic Science, Sungkyunkwan University, Suwon, Korea
[3]Department of Radiology, College of Medicine, Yonsei University, Seoul, Korea

Original Article

Received: December 21, 2016
Revised: January 20, 2017
Accepted: February 7, 2017

Correspondence to:
Dong-Hyun Kim, Ph.D.
Department of Electrical and Electronic Engineering, Yonsei University Room C228, Engineering Hall 3, Yonsei University, 50 Yonsei-ro, Seodaemun-gu Seoul 03722 Korea.
Tel. +82-2-2123-5874
Fax. +82-2-2123-2879
E-mail: donghyunkim@yonsei.ac.kr

Purpose: To investigate the exchange and redistribution of hyperpolarized ^{13}C metabolites between different pools by temporally analyzing the relative fraction of dual T_2* components of hyperpolarized ^{13}C metabolites.
Materials and Methods: A dual exponential decay analysis of T_2* is performed for [1-^{13}C] pyruvate and [1-^{13}C] lactate using nonspatially resolved dynamic ^{13}C MR spectroscopy from mice brains with tumors (n = 3) and without (n = 4) tumors. The values of shorter and longer T_2* components are explored when fitted from averaged spectrum and temporal variations of their fractions.
Results: The T_2* values were not significantly different between the tumor and control groups, but the fraction of longer T_2* [1-^{13}C] lactate components was more than 10% in the tumor group over that of the controls ($P < 0.1$). The fraction of shorter T_2* components of [1-^{13}C] pyruvate showed an increasing tendency while that of the [1-^{13}C] lactate was decreasing over time. The slopes of the changing fraction were steeper for the tumor group than the controls, especially for lactate ($P < 0.01$). In both pyruvate and lactate, the fraction of the shorter T_2* component was always greater than the longer T_2* component over time.
Conclusion: The exchange and redistribution of pyruvate and lactate between different pools was investigated by dual component analysis of the free induction decay signal from hyperpolarized ^{13}C experiments. Tumor and control groups showed differences in their fractions rather than the values of longer and shorter T_2* components. Fraction changing dynamics may provide an aspect for extravasation and membrane transport of pyruvate and lactate, and will be useful to determine the appropriate time window for acquisition of hyperpolarized ^{13}C images.

Keywords: Hyperpolarized ^{13}C; Metabolic imaging; T_2* relaxation time; [1-^{13}C] pyruvate; [1-^{13}C] lactate

INTRODUCTION

The discovery of the rapid dissolution dynamic nuclear polarization (DNP) technique has enabled real time imaging to reveal the kinetics of ^{13}C-labeled metabolites *in vivo* (1).

The most commonly used substrate in metabolic imaging to date is [1-^{13}C] pyruvate, especially in tumor metabolism (2). Following injection of hyperpolarized [1-^{13}C] pyruvate, increased [1-^{13}C] lactate signal was observed by rapid exchange of ^{13}C labeling between pyruvate and lactate (3) due to the high glycolytic rate of tumor characteristics (4). Intravenously injected [1-^{13}C] pyruvate is assumed to be predominantly in the intravascular space while the lactate is presumed to be largely in the intracellular space where the label exchange in the reaction catalyzed by the enzyme lactate dehydrogenase occurs (5). And a very rapid interconversion between lactate and pyruvate in blood has also been reported (6). Furthermore, during the label exchange of pyruvate and lactate, there is redistribution of metabolites via membrane transport or extravasation (Fig. 1).

Previously, apparent *in vivo* T_2 relaxation times of hyperpolarized [1-^{13}C] pyruvate and its downstream metabolites with multiple components were reported in several studies, which were measured from whole slices using a spin echo based method (7, 8). These T_2 data were acquired from a slice composed of various tissues including vasculature, which may explain the multiple T_2 components. In a study with simultaneous acquisition of the free induction decay (FID) and the spin echo signal, the extravascular species have been reported to have longer T_2 relaxation times than intravascular species (5).

Direct T_2 measurement is limited by the irreversible nature of the hyperpolarized signal. Multiple spin echo sequences such as the CPMG (Carr-Purcell-Meiboom-Gill) pulse (9) used for typical T_2 measurement cannot preserve the polarization after a single excitation. Therefore, the T_2 value can only be measured for a specific time point during the dynamic metabolic conversion.

While T_2 is a tissue intrinsic property for a certain metabolite, T_2* is an apparent constant depending on the extra magnetic field inhomogeneity. Tissues having the same T_2 can have different T_2* due to the influence of surrounding susceptibility environment. However, T_2* of a sample with multiple T_2 components would also have multiple components with same relative fractions with that of T_2 components. If the relative fractions of T_2 components are from intravascular and extravascular pools, investigation T_2* values with multiple components in time may be valuable to estimate the importance of extravasation or membrane transport on hyperpolarized ^{13}C metabolic kinetics.

Therefore, this work focused on the relative fraction of multiple T_2* components rather than T_2, to explore the temporal variation of their fractions. Nonspatially resolved dynamic ^{13}C magnetic resonance spectroscopy (MRS) of mouse brains was acquired at 9.4T and dual exponential decay analysis was performed for [1-^{13}C] pyruvate and [1-^{13}C] lactate signals extracted from acquired FID. The temporal change of the two components relative fractions was analyzed dynamically and the overall T_2* values from the averaged spectrum were also examined.

MATERIALS AND METHODS

Animal and Experimental Setup

Experiments were performed using four female BalB/C nude mice with brain tumors and three healthy female BalB/C nude mice as controls. 2×10^5 MDA-MB-231 human breast cancer cells were implanted stereotactically in the mice brains. *In vivo* dynamic ^{13}C MR experiments were performed 3 weeks after intracranial injection. The mice

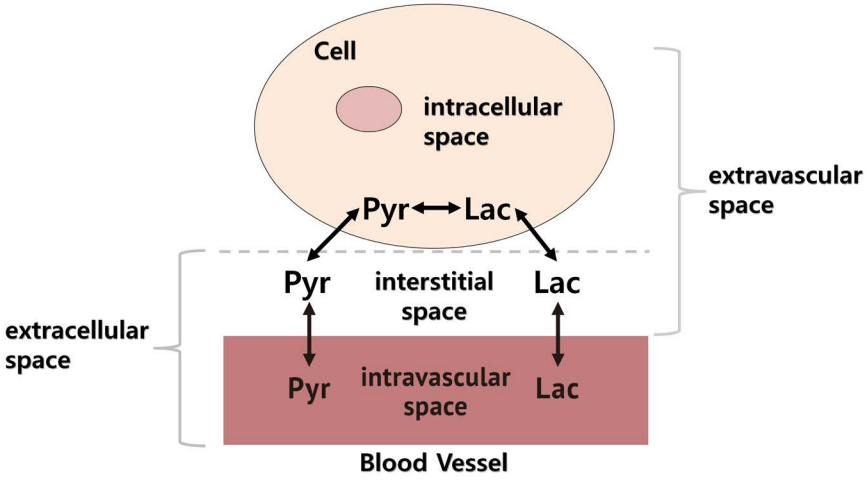

Fig. 1. Cellular spaces (metabolic pools) associated with exchange and redistribution of pyruvate and lactate.

were anesthetized by isoflurane (1-3%) inhalation and body temperature was maintained at 37℃ by a heating bed with circulating warm water during the scans. All procedures were approved by the local animal care and use committee.

For hyperpolarized ^{13}C experiments, [1-^{13}C] pyruvic acid (Cambridge Isotope, Tewksbury, MA, USA) doped with 15 mM Trityl radical OX-063 (Oxford instruments, Oxford, UK) and 1.5 mM Dotarem (Guerbet, Villepinte, France) was polarized via DNP technique using a HyperSense polarizer (Oxford Instruments, Oxford, UK). 3.8 mL of Tris/EDTA (trishydroxymethylaminomethane/ethylene diamine tetraacetic acid)-NaOH solution was used for dissolution, yielding a 75 mM solution of hyperpolarized [1-^{13}C] pyruvate with a pH of 7.5. Each mouse was injected with 350ul of the dissolved solution through a tail vein catheter.

MR Hardware and Pulse Sequence

All experiments were performed on a 9.4T Bruker BioSpec 94/20 USR small animal imaging system (Bruker BioSpin MRI GmbH, Ettlingen, Germany) equipped with a ^{1}H-^{13}C dual-tune surface coil (20 mm diameter).

For anatomical information, high resolution T_2 weighted turbo Rapid Acquisition with Refocused Echoes (RARE) ^{1}H images on the axial (Fig. 2a: field of view, 2 cm × 2 cm; matrix size, 128 × 128; 25 slices with 0.5 mm slice thickness) and coronal plane (Fig. 2b: field of view, 2.4 cm × 1.6 cm; matrix size, 160 × 104; 40 slices with 0.5 mm slice thickness) were acquired. Iterative 1st order B_0 shimming was performed locally over the mouse brain. The ^{13}C transmit gain was calibrated prior to each animal experiment using 8 M [1-^{13}C] urea syringe phantom placed near the mouse brain.

From the start of injection of hyperpolarized [1-^{13}C] pyruvate, a 10 mm axial slice including the brain tumor was acquired using a pulse-and-acquire sequence with a 0.25 ms slice selective Hermite pulse and with a flip angle of 10°. A 6510 Hz bandwidth spectrum of 2048 points was acquired dynamically every second over a period of 128 seconds.

Data Analysis

The raw FID was apodized in time domain by multiplying a decaying exponential function with a time constant of 100 ms for noise reduction (Fig. 2c), and Fourier transformed to a spectral domain. Phased spectra of pyruvate and lactate were extracted by Gaussian window with full width at half maximum of 300 Hz (Fig. 2d). Inverse Fourier transform of the extracted spectra were used for T_2^* decay analysis of the metabolites (Fig. 2e). The decay curves were first fitted using the non-negative least squares (NNLS) method (10) and two T_2^* components were consistently observed for both [1-^{13}C] pyruvate and [1-^{13}C] lactate from most of the dynamic spectra. Based on this result, decay curves were fitted using a nonlinear curve fitting algorithm (11) with the following dual exponential signal model with DC bias A:

$$S(t) = C_1 \exp\left(-\frac{t}{T_{2\,(1)}^*}\right) + C_2 \exp\left(-\frac{t}{T_{2\,(2)}^*}\right) + A \qquad [1]$$

where $T_{2\,(1)}^*$ and $T_{2\,(2)}^*$ are the apparent T_2^* variables, and C_1 and C_2 are the corresponding weighting factors.

Finally, the estimated T_2^* values were corrected with the apodization taken into account:

$$\frac{1}{T_{2\,C}^*} = \frac{1}{T_{2\,F}^*} - \frac{1}{100(\text{ms})} \qquad [2]$$

where $T_{2\,C}^*$ is corrected estimation of T_2^* and $T_{2\,F}^*$ is fitted T_2^* using Eq. [1].

Decay curves from the averaged spectrum were fitted to investigate the overall T_2^* values and curves from the spectrum of each single time point were fitted to analyze the tendency for temporal change of relative fractions. A five time point moving average was used to fit the [1-^{13}C] lactate signal to assure sufficient signal to noise ratio (SNR) for fitting accuracy. The fitting interval was set to the time points that had reliable fitting results, meaning that the fittings did not diverge.

The data analysis was performed using MATLAB (R2012a, MathWorks, Natick, MA, USA).

RESULTS

Averaged Spectrum Analysis

Figure. 3 shows the T_2^* value results (Fig. 3a) and their relative fractions (Fig. 3b) from the averaged tumor and control group spectra. The T_2^* values and fraction of [1-^{13}C] pyruvate from the average of all spectra in the fitting interval were 4.04 ± 1.67 ms (80 ± 3%) and 28.59 ± 11.55 ms (20 ± 3%) for tumor group (n = 4) and 3.19 ± 0.95 ms (85 ± 8%) and 26.45 ± 6.16 ms (15 ± 8%) for control group (n = 3). For [1-^{13}C] lactate, the T_2^* values and the fraction of tumor group were 2.62 ± 0.73 ms (65 ± 9%) and 17.64

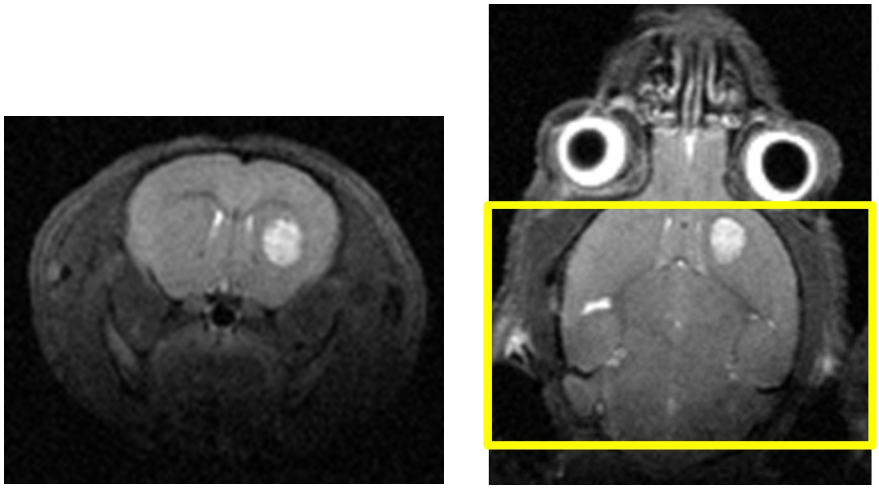

a b

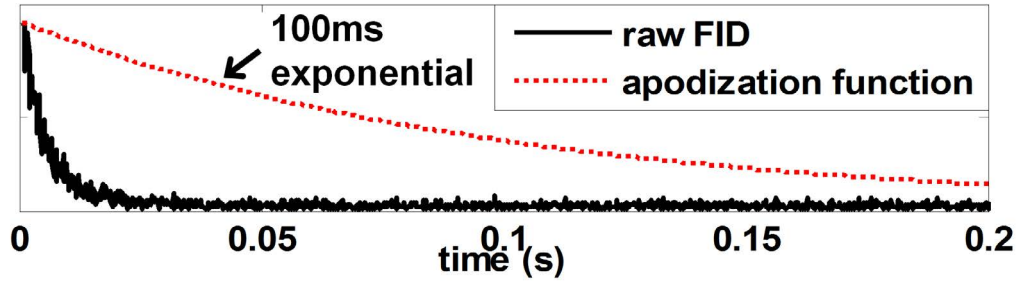

c

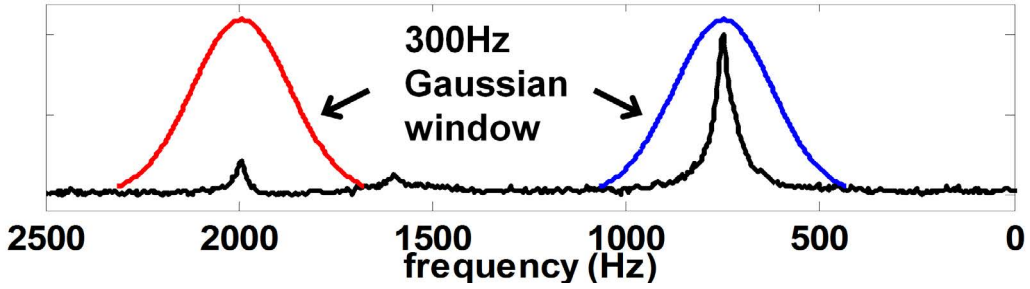

d

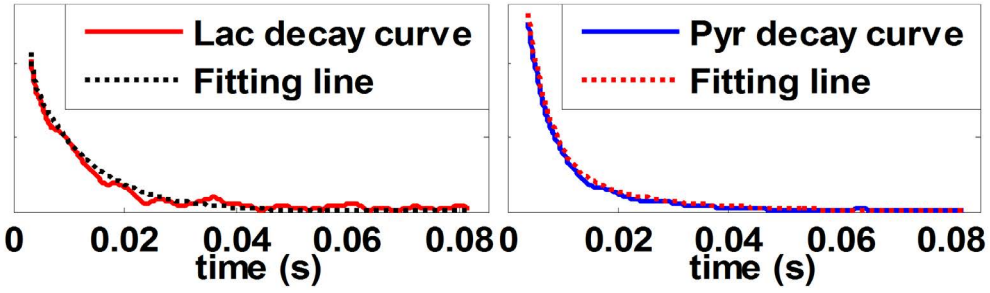

e

Fig. 2. ^1H T_2 weighted anatomical images on (a) axial and (b) coronal slices. The yellow box indicates the slice of excitation. (c) Time domain apodization with 100 ms decaying exponential, (d) 300 Hz Gaussian window in spectral domain, (e) extracted decay curves of lactate (enlarged) and pyruvate with its fitting line.

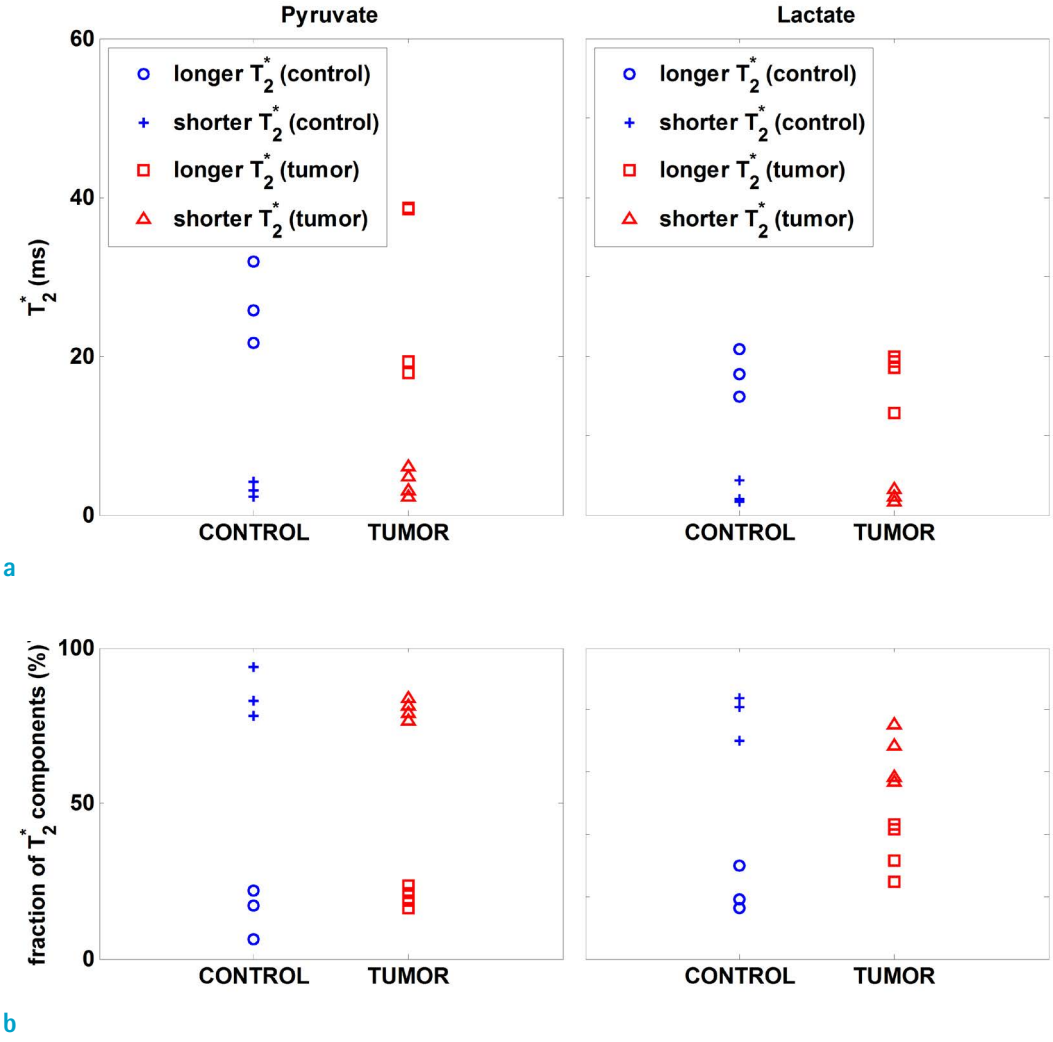

Fig. 3. (a) T_2* values and (b) their relative fraction of [1-^{13}C] pyruvate and lactate of averaged spectrum.

± 3.25 ms (33 ± 9%), and those of the control group were 2.65 ± 1.42 ms (78 ± 7%) and 17.80 ± 3.02 ms (22 ± 7%). The T_2* values were not significantly different between the tumor and control groups (P = 0.8767), but the mean value of the relative fraction of the longer T_2* lactate component was more than 10% greater in the tumor group than that of the controls (P < 0.1). On the other hand, the fractional difference of the T_2* components of pyruvate between the tumor and control groups had a P-value of 0.3198.

Dynamic Spectra Analysis

The inter-subject mean and standard deviation of T_2* values and their fractions are shown in a time course in Figure. 4a and b, respectively. The time axis was matched by the start of injection and only data from overlapped fitting intervals were used. Throughout the studies, the fraction of the shorter T_2* [1-^{13}C] pyruvate component showed an increasing tendency, and that of [1-^{13}C] lactate decreased over time. The slopes of the changing fraction for lactate were steeper for the tumor group than the controls with significance of P < 0.01. For pyruvate, the temporal change of fraction showed a similar tendency with lactate, but the slopes were not significantly different between the tumor and control groups (P = 0.1306). In both pyruvate and lactate, the fraction of the shorter T_2* component was always greater than the longer T_2* component over the time frame.

Figure. 4c represents the dynamic signals of [1-^{13}C] pyruvate and lactate, showing the total as well as the shorter and longer T_2* components of the tumor and control groups. Each dynamic curve was normalized by the maximum intensity of pyruvate signal. The intensity of the

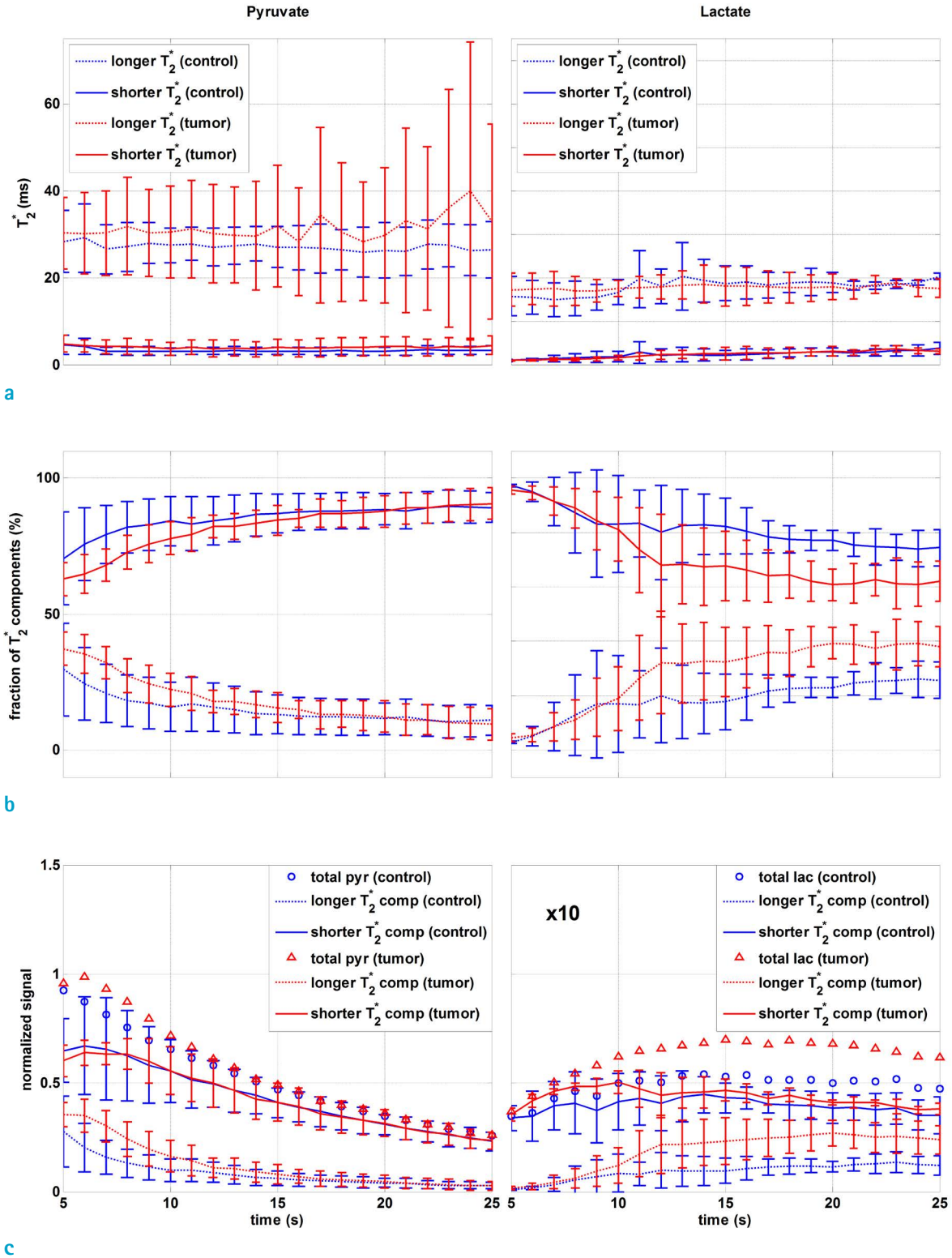

Fig. 4. Temporal change of (a) T_2* values [1-^{13}C] pyruvate and lactate and (b) their relative fractions for the tumor (red) and control (blue) groups. (c) Dynamic signals of [1-^{13}C] pyruvate and lactate, showing the total, shorter and longer T_2* components of the tumor and control groups. Each dynamic curve was normalized by maximum pyruvate signal intensity. Mean and standard deviation of inter-subject signal are indicated. Injection started at t = 0.

longer T_2* component of lactate signal was initially very small in both tumor and control groups. The total lactate signal was higher in the tumor group than the control group.

DISCUSSION AND CONCLUSION

A dual component assessment of *in vivo* T_2* decay of [1-^{13}C] pyruvate and [1-^{13}C] lactate and a temporal analysis of the relative fraction of the dual T_2* were presented. The overall T_2* values, which were not significantly different between the tumor and control groups, indicate that the T_2* of ^{13}C metabolites are dominantly affected by the field inhomogeneity rather than the intrinsic T_2 value. However, the difference in relative fraction of the longer T_2* [1-^{13}C] lactate component was more than 10% greater in the tumor group than the control with significance of $P < 0.1$. Assuming that the longer T_2* component, as in the case of the reported T_2 value (5), is from intracellular or extravascular species, this can be explained by elevated isotope exchange in the tumor due to the large endogenous lactate pool.

In dynamic spectra analysis, the FID acquisition time at each time point was 315 ms. However, the effective acquisition time was less than 100 ms since the FID signal length was limited to T_2*. Given that the reported rate constants Kp values are rarely greater than 0.1 s^{-1}, this is sufficient time to capture the instantaneous amount of metabolite.

The fraction of the shorter T_2*[1-^{13}C] pyruvate component during the fitting interval was always greater than the longer T_2* component. Considering that spatially resolved chemical shift imaging results commonly show concentrated pyruvate signals in the blood vessel (12), this is also consistent with the assumption that the T_2* of intravascular species has a shorter value. The increase in the shorter T_2* pyruvate component fraction over time implies that the influx of injected pyruvate into the excitation slice is more dominant than the extravasation or cell uptake of pyruvate.

Meanwhile, the longer T_2* component of [1-^{13}C] lactate signal was initially very small but increased in fraction as well as signal intensity over time. This reflects the newly generated ^{13}C-labeled lactate signal in the intracellular space as a result of isotope exchange between pyruvate and endogenous lactate. It is presumed that the shorter T_2* [1-^{13}C] lactate component signal having a large fraction from the beginning was from ^{13}C-labeled lactate introduced from blood or other tissues outside the excitation slice. The total [1-^{13}C] lactate signal was higher in the tumor group. Also, the increase of the longer T_2* lactate component fraction was steeper compared to the control. This is also consistent with the presumption that the longer T_2* component is from intracellular species in tumors that exhibit higher exchange rates than normal tissues.

We found that the fraction of T_2* lactate components was significantly different between the tumor and control groups for both averaged spectrum analysis and dynamic spectra analysis, while that of pyruvate did not have a statistically significant difference. This result may be due to the small sample size, or that the tumor used in the experiments was not perfused much, due to the lack of vascularization.

It might be premature to conclude that the longer and shorter T_2* components respectively come from the extravascular and intravascular species due to the limitations of a whole slice study. The data was composed of signals from other types of tissues and the tumor was only a small volume of the entire excitation slice (~3% of the brain volume in slice). *In vivo* experiments using a subcutaneous tumor model and/or surface coil with more localized sensitivity, or *in vitro* experiments with a cell line, might be needed for more precise evaluation of multiple T_2* components. Techniques used to investigate the exchange process, such as magnetization transfer, could also be helpful. This preliminary study suggests an analysis method to further investigate exchange and redistribution between different pools.

Acknowledgments

This research was supported by a grant of the Korea Health Technology R&D Project through the Korea Health Industry Development Institute (KHIDI), funded by the Ministry of Health & Welfare, Republic of Korea (grant number : HI15C2422).

REFERENCES

1. Ardenkjaer-Larsen JH, Fridlund B, Gram A, et al. Increase in signal-to-noise ratio of > 10,000 times in liquid-state NMR. Proc Natl Acad Sci U S A 2003;100:10158-10163
2. Kurhanewicz J, Vigneron DB, Brindle K, et al. Analysis of cancer metabolism by imaging hyperpolarized nuclei: prospects for translation to clinical research. Neoplasia

2011;13:81-97
3. Day SE, Kettunen MI, Gallagher FA, et al. Detecting tumor response to treatment using hyperpolarized 13C magnetic resonance imaging and spectroscopy. Nat Med 2007;13:1382-1387
4. Warburg O. On the origin of cancer cells. Science 1956;123:309-314
5. Kettunen MI, Kennedy BW, Hu DE, Brindle KM. Spin echo measurements of the extravasation and tumor cell uptake of hyperpolarized [1-(13) C]lactate and [1-(13) C]pyruvate. Magn Reson Med 2013;70:1200-1209
6. Romijn JA, Chinkes DL, Schwarz JM, Wolfe RR. Lactate-pyruvate interconversion in blood: implications for in vivo tracer studies. Am J Physiol 1994;266:E334-340
7. Yen YF, Le Roux P, R. Bok R, et al. Apparent T2 of 13C-labeled metabolites in vivo. In Proceedings of the 16th Annual Meeting of ISMRM. Toronto: Canada, 2008:1747
8. Kettunen MI, Hu DE, Witney TH, et al. Magnetization transfer measurements of exchange between hyperpolarized [1-13C]pyruvate and [1-13C]lactate in a murine lymphoma. Magn Reson Med 2010;63:872-880
9. Carr HY, Purcell EM. Effects of diffusion on free precession in nuclear magnetic resonance experiments. Phys Rev 1954;94:630-638
10. Whittall KP, Mackay AL. Quantitative interpretation of NMR relaxation data. J Magn Reson 1969;84:134-152
11. Coleman TF, Li Y. An interior trust region approach for nonlinear minimization subject to bounds. SIAM J Optim 1996;6:418-445
12. Hurd RE, Yen YF, Mayer D, et al. Metabolic imaging in the anesthetized rat brain using hyperpolarized [1-13C] pyruvate and [1-13C] ethyl pyruvate. Magn Reson Med 2010;63:1137-1143